STATION-KEEPING STRATEGIES FOR LIBRATION POINT ORBITS: TARGET POINT AND FLOQUET MODE APPROACHES

K. C. Howell* and T. M. Keeter†

Spacecraft in orbits near the interior libration point in the Sun-Earth system are excellent platforms for scientific investigations concerning solar effects on the terrestrial environment. Since such libration point trajectories are generally unstable, spacecraft moving on such paths must use some form of trajectory control to remain close to their nominal orbit. The long-term goal of this effort is the development of station-keeping strategies applicable to such trajectories. Two approaches serve as the focus of the current discussion. The Target Point strategy and the Floquet Mode approach both use maneuvers executed (impulsively) at discrete time intervals. The analysis includes some investigations of a number of the problem parameters that affect the overall cost. Simulations are designed to provide representative costs for a spacecraft moving in a libration point trajectory; preliminary results are summarized.

INTRODUCTION

A number of missions proposed for launch over the next decade are likely to employ halo or Lissajous orbits in the vicinity of the interior L_1 libration point of the Sun–Earth/Moon barycenter system. This effort is directed toward the development of two particular station-keeping approaches that can be used to maintain spacecraft near such libration point trajectories. A longer term goal is a direct comparison of the methods. However, even the preliminary results indicate that each type of analysis offers unique insights into the problem that may be mutually beneficial.

Halo and Lissajous orbits are solutions that represent bounded motion in the vicinity of a collinear libration point. The problem of controlling a spacecraft moving on an (inherently unstable) libration point orbit is receiving increasing attention. In the late 1960s, Farquhar [1] suggested several station-keeping strategies for nearly–periodic solutions near the collinear points. Later, in 1974, a station-keeping method for spacecraft moving on halo orbits in the vicinity of the Earth-Moon translunar libration point (L_2) was published by Breakwell et al. [2] In contrast, specific mission requirements influenced the station-keeping strategy for the first libration point mission. Launched in 1978, the International Sun–Earth Explorer–3 (ISEE–3) spacecraft remained in a near–halo orbit associated with the interior libration point (L_1) of the Sun–Earth/Moon barycenter system for approximately three and a half years [3]. Impulsive maneuvers at discrete time intervals (up to 90 days)

* Associate Professor, School of Aeronautics and Astronautics, Purdue University, 1282 Grissom Hall, West Lafayette, Indiana 47907-1282.

† Graduate Student, School of Aeronautics and Astronautics, Purdue University, West Lafayette, Indiana. Currently with Dynetics, Inc., P.O. Drawer B, Huntsville, Alabama 35814-5050.

were successfully implemented as a means of trajectory control. Since that time, more detailed investigations have resulted in various station-keeping strategies, including the two identified here as the Target Point and Floquet Mode approaches.

The Target Point method computes corrective maneuvers by minimizing a weighted cost function [4, 5]. The cost function is defined in terms of a corrective maneuver as well as position and velocity deviations from the nominal orbit at a number of specified future times t_i. The nominal state vectors at each time t_i are denoted as "target points." The target points are selected along the trajectory at discrete time intervals that are downstream of the maneuver. The Floquet Mode approach, as discussed by Simó, Gómez, Llibre, and Martínez [6, 7], incorporates invariant manifold theory and Floquet modes to compute the maneuvers. The basic concept is relatively straightforward in the context of the circular restricted three-body problem (CR3BP) and the assumption of a periodic trajectory. Floquet modes associated with the monodromy matrix are used to determine the unstable component corresponding to the local error vector. The maneuver is then computed such that it eradicates the dominant unstable component of the error. It is noted that the Floquet Mode approach has also been demonstrated in a model that is more complex than that associated with the circular restricted problem.

THE SUN–EARTH–MOON MODEL AND NOMINAL ORBIT

In previous studies, halo and Lissajous trajectories have been numerically determined from exact nonlinear differential equations using differential corrections schemes. The dynamic model adopted here is identified as the Sun–Earth–Moon model (SEM) and includes (only) the gravitational influences of the Sun, Earth, and Moon on the spacecraft. The locations of the Sun and Moon with respect to the Earth are computed from polynomial series representations of ephemeris data. The simulation algorithm is general in nature such that it can be easily expanded to include force models for additional perturbing forces (e.g., other attracting bodies and solar radiation pressure).

For this investigation, a nominal halo orbit is defined in the Sun–Earth–Moon system and is similar in size to the halo trajectory previously employed in the ISEE–3 mission and investigated in connection with the Solar and Heliospheric Observatory (SOHO) mission. The plot in Fig. 1 includes three orthographic projections of the nominal halo trajectory used in this investigation. Although computations are done in cartesian coordinates, it is desirable to display trajectories in terms of coordinates corresponding to the usual rotating frame with origin at L_1. The three axes associated with the figure are then defined consistent with the rotating frame typically used with the restricted three-body problem. Thus, the x axis is directed from the larger primary (Sun) to the smaller (Earth/Moon barycenter), the y axis is defined in the plane of the orbit of the primaries 90° from the x axis, and the z axis completes the right-handed frame. The orbit is plotted relative to L_1, but the L_1 point does not actually exist in the Sun–Earth–Moon system in the same sense that it does in the restricted problem since the motion of the primaries is not periodic and includes three gravity fields. Figure 1 is accomplished by using the known location of L_1 in the elliptic restricted problem to compute a corresponding approximate location for the libration point in the system defined by the SEM model. Note that the trajectory is classified as a "southern" orbit. A total of 14 revolutions are shown that translate to a 6.33 year trajectory. Arrows are included in the x–y and y–z projections to indicate the

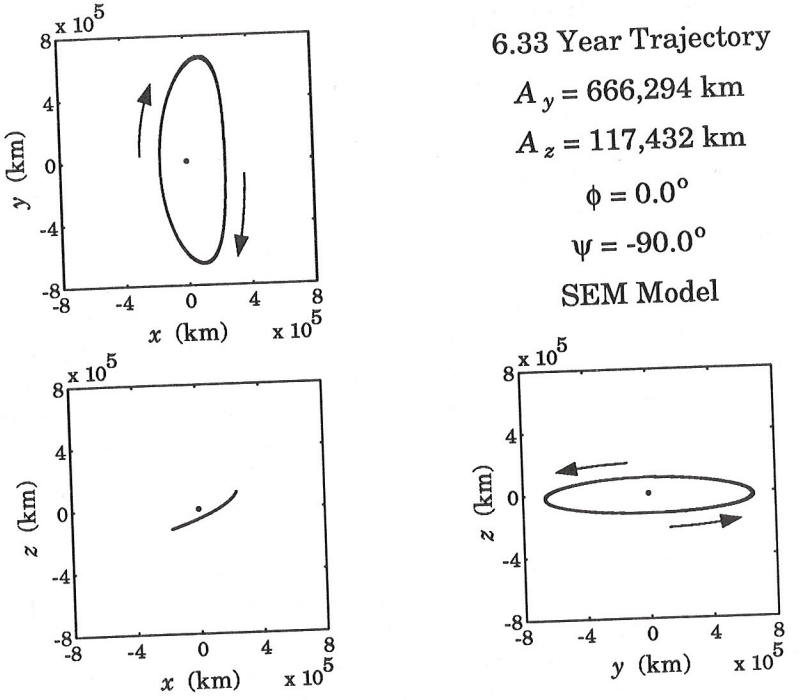

Figure 1: Near–Halo Trajectory Selected as Nominal Path

direction of spacecraft motion. For computational convenience, the initial epoch is selected as the minimum z–location.

For both station–keeping strategies developed here, the nominal orbit and its state transition matrix (STM) must be available at any time along the orbit in a computationally convenient manner. Inaccurate representations contribute to higher maneuver costs. From a number of options, the most accutate method employs a technique that represents the nominal orbit by an Akima cubic spline interpolation. Storing the nominal path in this form provides a very accurate and convenient representation if the data points are spaced in intervals less than or equal to 1.1 days. Unfortunately, the size of the data files precludes the use of this method to represent the 36 elements of the state transition matrix. Rather than attempt to represent each element, the simulation software will reproduce the state transition matrix associated with the nominal orbit, as needed, by numerically integrating the variational equations assuming primary motion consistent with the SEM model. It is noted that this approach depends heavily on an accurate representation of the nominal orbit.

THE STATION–KEEPING PROBLEM

Definition

Once the nominal libration point orbit is specified, strategies must be implemented to maintain the actual spacecraft trajectory sufficiently close to the nominal path, i.e., within a region that is locally approximated as a torus of some specified radius centered about the "reference" path. It is not required that the spacecraft remain precisely on the nominal path. Thus, the goal of the station-keeping process is to compute and implement maneuvers to maintain a vehicle within the acceptable region defined by the torus. All maneuvers are assumed to be impulsive and occur at discrete times. Overall, the objective of this investigation is threefold: (i) At a given time, evaluate the necessity of a station-keeping maneuver. (ii) If a maneuver is necessary, compute the magnitude and direction of the $\Delta\bar{v}$. (iii) For the duration of the mission, optimize the timing and magnitudes of the corrective maneuvers to minimize the total cost.

To evaluate various station-keeping strategies, a numerical simulation algorithm is employed to compute the spacecraft trajectory under the influence of the modeled forces and to calculate the "instantaneous" changes in the trajectory resulting from discrete station-keeping maneuvers. For the simulation algorithm used in this study, no attempt has been made to include all of the conditions that could affect the spacecraft's actual trajectory. The simulation algorithm has been developed solely to provide a tool that could be used to evaluate possible station–keeping strategies. The focus has thus been restricted to consideration of the impact of the injection, tracking, and maneuver processes on a nominal orbit determined in the presence of gravity from the Sun, Earth, and Moon.

Target Point Approach

Previous work [4, 5] has resulted in the development of a control procedure that is derived from minimization of a cost function. The cost function, J, is defined by weighting both the control energy required to implement a station-keeping maneuver, $\Delta\bar{v}$, and a series of predicted deviations of the six–dimensional state from the nominal orbit at specified future times. Thus, the cost function simplifies to the form

$$J = \Delta\bar{v}^T\mathcal{Q}\Delta\bar{v} + \bar{p}_1^T\mathcal{R}\bar{p}_1 + \bar{v}_1^T\mathcal{R}_v\bar{v}_1 + \bar{p}_2^T\mathcal{S}\bar{p}_2 + \bar{v}_2^T\mathcal{S}_v\bar{v}_2 + \bar{p}_3^T\mathcal{T}\bar{p}_3 + \bar{v}_3^T\mathcal{T}_v\bar{v}_3 \,, \qquad (1)$$

where superscript T denotes transpose. The variables in the cost expression include the corrective maneuver, $\Delta\bar{v}$ at some time t_c. Then $\bar{p}_1$, $\bar{p}_2$, and $\bar{p}_3$ are defined as 3×1 column vectors representing linear approximations of the expected position deviations of the actual spacecraft trajectory from the nominal path (if no corrective action is taken) at specified future times t_1, t_2, and t_3, respectively. Likewise, the 3×1 vectors $\bar{v}_1$, $\bar{v}_2$, and $\bar{v}_3$ represent deviations of the spacecraft velocity at the corresponding time t_i. (Both position and velocity residuals relative to the nominal trajectory make a contribution to spacecraft drift so both are included in the state propagation equation.) The future times at which predictions of the position and velocity state of the vehicle are compared to the nominal path are denoted as the target points. The choice of identifying *three* future target points is arbitrary.

In Eqn. (1), $\mathcal{Q}$, $\mathcal{R}$, $\mathcal{S}$, $\mathcal{T}$, $\mathcal{R}_v$, $\mathcal{S}_v$, and $\mathcal{T}_v$ are 3×3 weighting matrices. The weighting matrices are generally treated as constants that must be specified as inputs. Selection

of appropriate weighting matrix elements is a trial and error process that is quite time–consuming. A methodology has been developed that automatically selects and updates the weighting matrices for each maneuver. This "time–varying" weighting matrix algorithm is based purely on empirical observations. Also, the performance of the modified Target Point algorithm is not yet "optimal," though it has been demonstrated to successfully control the spacecraft at relatively low costs. This accomplishment alone provides the user with a quick and efficient way to obtain reasonable station-keeping results. Given some procedure to select the weighting matrices, the "optimal" maneuver is therefore computed by minimizing the cost function, J. The resulting corrective maneuver ($\Delta\bar{v}_{min}$) is a function of spacecraft drift (in both position and velocity with respect to the nominal orbit), state transition matrix elements associated with the nominal orbit (through the state propagation equation), and the weighting matrices [5]. It is assumed here that there is no delay in implementation of the maneuver; the corrective maneuvers occur at time t_o, defined as the current time. Note that this general method could certainly accommodate the inclusion of additional target points.

Numerous station–keeping simulations implementing the Target Point approach have been performed for the nominal orbit in Fig. 1. Three additional constraints are specified in the station-keeping procedure that impact the timing of each maneuver. First, the time elapsed between successive maneuvers must be greater than or equal to a specified minimum time interval, t_{min}. This constraint may be due to the orbit determination requirements, scientific payload requirements, and/or mission operations. The second constraint is a scalar distance (p_{min}) and specifies a minimum drift from the nominal path (an isochronous correspondence) that must be exceeded prior to maneuver execution. For distances less than p_{min}, maneuver computations do not occur. Third, in the station-keeping simulation, the magnitude of position deviations are compared between successive tracking intervals. If the magnitude is decreasing, a maneuver is not computed. For a corrective maneuver to be computed, all three criteria must be satisfied simultaneously.

After a maneuver is calculated by the algorithm, an additional constraint is specified on the minimum allowable maneuver magnitude, v_{min}. If the magnitude of the calculated $\Delta\bar{v}$ is less than v_{min}, then the recommended maneuver is cancelled. This constraint is useful in avoiding "small" maneuvers that are approximately the same order of magnitude as the maneuver errors. It also serves to model any actual hardware limitations.

Floquet Mode Approach

An alternate strategy for station–keeping is the Floquet Mode approach [6, 7], a method that significantly differs from the Target Point method. Conceptually, it can be formulated in the CR3BP. In this context, primary motion as well as the nominal halo orbit can be assumed periodic. The variational equations for motion in the vicinity of the nominal trajectory will then be linear with periodic coefficients. Thus, in general, both qualitative and quantitative information can be obtained about the behavior of the nonlinear system from the eigenvalues and eigenvectors of the state transition matrix (STM).

Recall that the STM $\Phi(t, t_o)$ is available at any time t along the nominal path. Given a spacecraft orbit that is periodic, (i.e., a halo orbit), all revolutions along the path are identical by comparison. Thus, one isolated revolution, and information obtained from it, is a sufficient representation of the entire trajectory. Let $M(\mathbb{P}+t_o)$ denote the mon-

odromy matrix, that is, the STM matrix after one full revolution along the (periodic) halo orbit. (For quasi-periodic orbits such as halo orbits in the elliptic restricted problem or the SEM system, the trajectory will never retrace itself exactly. Nevertheless, development of the methodology in the context of a perfectly periodic orbit is adequate, concurrent with adjustments in the numerical implementation.) Behavior of the solution for the linear (variational) system, then, is determined by the eigenvalues of the 6×6 monodromy matrix. Again assume that the nominal trajectory is a periodic halo orbit in the CR3BP. A unique set of characteristic (Floquet) multipliers or roots can be determined; they exist as reciprocal pairs. Of the six, it is well known that one eigenvalue (λ_1) is real and greater than one, one (λ_2) is real and less than one, and four are on the unit circle (λ_3, λ_4, λ_5, and λ_6). Two of the neutral eigenvalues, λ_3 and λ_4, are real and equal to one. The other two neutral eigenvalues, λ_5 and λ_6, are actually a complex conjugate pair, each with a modulus equal to unity. Thus, λ_1 is the dominant eigenvalue and is associated with the unstable nature of the collinear libration points. The corresponding eigenvector, $\bar{e}_1(\mathbb{P}+t_o)$, represents the dominant, exponential divergence from the vicinity of the halo orbit. To maintain the spacecraft near the nominal orbit, the influence of this divergent character on the motion of the spacecraft must be effectively minimized by control maneuvers.

For implementation of this station-keeping approach, information about the behavior of the vehicle – in terms of the eigenvectors – is available at all times by employing Floquet modes. They are obtained directly from the STM through the expression

$$\tilde{E}(t,0) = \Phi(t,0)\, S e^{-\tilde{J}t}\,. \tag{2}$$

Assuming $t_o = 0$, $\tilde{E}(t,0)$ is a periodic matrix containing the Floquet modes associated with the STM $\Phi(t,0)$, S is a real, square matrix containing the eigenvectors of the monodromy matrix, and $\tilde{J}$ is a real matrix with block diagonal elements defined in terms of the Poincaré exponents associated with $M(\mathbb{P})$.

From Eqn. (2), the Floquet modes can be obtained for any point along the nominal trajectory and the control algorithm is developed to utilize this information for station–keeping purposes (with suitable numerical adjustments). Theoretical emphasis is placed on formulating a controller that will effectively eliminate the unstable component of a 6-dimensional error vector, $\bar{\delta}(t)$. The error is defined as the difference between the "actual" position and velocity states and the desired states corresponding to the predefined nominal path at time t. The error vector $\bar{\delta}(t)$ is comprised of six elements,

$$\bar{\delta}(t) = [\delta x(t), \delta y(t), \delta z(t), \delta x'(t), \delta y'(t), \delta z'(t)]^T, \tag{3}$$

where T implies transpose and primes indicate differentiation with respect to time. The elements are currently expressed in terms of rotating, libration point–centered coordinates. The vector $\bar{\delta}(t)$ as defined in Eqn. (3), represents the error in six-dimensional state–space. Correspondingly, at time t, the eigenbasis obtained from the Floquet modes, $\tilde{E}(t,0)$, is similarly associated with the state–space.

By projecting $\bar{\delta}$ onto $\tilde{E}$, the vector $\bar{\delta}$ will be resolved into six components associated with the Floquet basis, $\bar{\tilde{e}}_i$. This is accomplished by multiplying $\bar{\delta}$ by projection matrices such that

$$\bar{\delta}_i = \Pi_i\, \bar{\delta}, \tag{4}$$

where

$$\Pi_i = \frac{\bar{\tilde{e}}_i \bar{\tilde{e}}_i^T}{\bar{\tilde{e}}_i^T \bar{\tilde{e}}_i} . \tag{5}$$

The projection matrices, Π_i, are 6×6 symmteric matrices with the property

$$\Pi_i{}^{2n} = \Pi_i{}^{n}. \tag{6}$$

Therefore, the expression

$$\bar{\delta}_1 = \Pi_1 \bar{\delta}, \tag{7}$$

produces the component of $\bar{\delta}$ in the unstable direction. Note that the unstable component vector $\bar{\delta}_1$ can be expressed in terms of any six-dimensional basis. The operation in Eqn. (4) will produce the $\bar{\delta}_i$ as vectors represented in terms of state–space coordinates, i.e.,

$$\bar{\delta}_i = [\delta_{i_x}, \delta_{i_y}, \delta_{i_z}, \delta_{i_{x'}}, \delta_{i_{y'}}, \delta_{i_{z'}}]^T, \tag{8}$$

where the subscripts x, y, z, x', y', and z' indicate the corresponding state–space component. Conceptually, the error vector has been rewritten in terms of eigenbasis components, i.e.,

$$\bar{\delta}(t) = C_1 \hat{u}_1 + C_2 \hat{u}_2 + \cdots + C_6 \hat{u}_6 , \tag{9}$$

where, for example,

$$C_1 = |\bar{\delta}_1| . \tag{10}$$

Thus, $\hat{u}_1$ corresponds to the unstable direction. (The Floquet modes represented by the eigenbasis vectors $\bar{\tilde{e}}_i$ are generally not orthogonal; thus, neither are the components $\bar{\delta}_i$ orthogonal. For implementation, a partial orthogonalization is required that produces a basis with all $\hat{u}_i$, i = 2,3,...,6, orthogonal to $\hat{u}_1$.)

In the design of the controller, the objective is the elimination of $\bar{\delta}_1$ by implementing a maneuver,

$$\Delta\bar{V} = \left\{ \begin{array}{c} 0 \\ - - - \\ \Delta\bar{v} \end{array} \right\} = [0, 0, 0, \Delta_x, \Delta_y, \Delta_z]^T, \tag{11}$$

where Δ_x, Δ_y, and Δ_z are the x, y, and z velocity components of the three-element maneuver vector $\Delta\bar{v}$. Thus, the controller objective is mathematically represented by the expression

$$\bar{\delta}(t) + \Delta\bar{V} = \bar{\Delta}(t), \tag{12}$$

where

$$\bar{\Delta}(t) = a_2 C_2 \hat{u}_2 + a_3 C_3 \hat{u}_3 + \cdots + a_6 C_6 \hat{u}_6 . \tag{13}$$

and a_i =constant, i = 2,3,...6. Note that the unstable component has been eliminated on the right hand side of Eqn. (12). The expression for the controller can be reduced to a more convenient form by subtracting the $\hat{u}_2$ through $\hat{u}_6$ components of $\bar{\delta}$ from both sides of Eqn. (12) such that

$$\bar{\delta}_1 + \Delta\bar{V} = \alpha_2 C_2 \hat{u}_2 + \alpha_3 C_3 \hat{u}_3 + \cdots + \alpha_6 C_6 \hat{u}_6 , \tag{14}$$

where the unknown elements α_i on the right side of the equation are constant and defined as

$$\alpha_i = a_i - 1. \tag{15}$$

Expanded in terms of state–space components, the control algorithm can be mathematically represented as follows,

$$\begin{Bmatrix} \delta_{1_x} \\ \delta_{1_y} \\ \delta_{1_z} \\ \delta_{1_{x'}} \\ \delta_{1_{y'}} \\ \delta_{1_{z'}} \end{Bmatrix} + \begin{Bmatrix} 0 \\ 0 \\ 0 \\ \Delta_x \\ \Delta_y \\ \Delta_z \end{Bmatrix} = \begin{bmatrix} \delta_{2_x} & \delta_{3_x} & \cdots & \delta_{6_x} \\ \delta_{2_y} & & & \\ \delta_{2_z} & & & \\ \delta_{2_{x'}} & \vdots & \ddots & \vdots \\ \delta_{2_{y'}} & & & \\ \delta_{2_{z'}} & \delta_{3_{z'}} & \cdots & \delta_{6_{z'}} \end{bmatrix} \begin{Bmatrix} \alpha_2 \\ \alpha_3 \\ \alpha_4 \\ \alpha_5 \\ \alpha_6 \end{Bmatrix} . \tag{16}$$

Thus, the three components of the maneuver vector $\Delta\bar{v}$ that are required to eliminate the unstable component of the error are determined from Eqn. (16).

The simplest solution to Eqn. (16) is obtained if maneuvers are restricted to only one direction. The system of equations then admits five constraint equations and five unknowns, so the unidirectional maneuver has only one solution. Of the three potential directions, the x–direction has clearly proven to be the most effective. A three–axis controller can also be formulated from Eqn. (16) by simultaneously solving for all five α_i and three $\Delta\bar{v}$ components and minimizing a suitable norm. Rewriting Eqn. (16) such that all scalar unknowns appear in one eight–element vector $\bar{\alpha}^*$,

$$\bar{\delta}_1 = \left[\begin{array}{cccc|ccc} \delta_{2_x} & \delta_{3_x} & \cdots & \delta_{6_x} & 0 & 0 & 0 \\ \delta_{2_y} & & & & 0 & 0 & 0 \\ \delta_{2_z} & \vdots & \ddots & \vdots & 0 & 0 & 0 \\ \delta_{2_{x'}} & & & & -1 & 0 & 0 \\ \delta_{2_{y'}} & & & & 0 & -1 & 0 \\ \delta_{2_{z'}} & \delta_{3_{z'}} & \cdots & \delta_{6_{z'}} & 0 & 0 & -1 \end{array}\right] \begin{Bmatrix} \alpha_2 \\ \alpha_3 \\ \alpha_4 \\ \alpha_5 \\ \alpha_6 \\ \Delta_x \\ \Delta_y \\ \Delta_z \end{Bmatrix} , \tag{17}$$

or

$$\bar{\delta}_1 = \tilde{E}^* \bar{\alpha}^* . \tag{18}$$

From a number of possibilities, the norm is defined as

$$\min_{\bar{\alpha}^*} \|\bar{\alpha}^*\|_Q{}^2 , \tag{19}$$

subject to the constraint

$$g(\bar{\alpha}^*) = \tilde{E}^* \bar{\alpha}^* - \bar{\delta}_1 = 0 . \tag{20}$$

The weighting matrix, Q, is added to Eqn. (19) to provide greater flexibility. Then the resulting expression,

$$\bar{\alpha}^* = Q^{-1} \tilde{E}^{*T} (\tilde{E}^* Q^{-1} \tilde{E}^{*T})^{-1} \bar{\delta}_1 , \tag{21}$$

provides a solution.

The Floquet strategy based in Eqn. (16) is implemented using the station–keeping algorithm previously described. Similar to implementation of the Target Point strategy, additional constraints that are specified will also impact the timing of each maneuver. In addition to a minimum time interval between maneuvers (t_{min}) and a minimum computed maneuver magnitude (v_{min}) as defined for the Target Point method, two additional constraints are specified that directly influence the implementation of corrective maneuvers

using the Floquet Mode approach. Previously, p_{min} was defined as a minimum drift to be exceeded prior to maneuver implementation. The corresponding quantity here is a minimum magnitude for the unstable component of the error vector that is specified as $|\bar{\delta}_1|_{min}$; the value is selected to correspond to the expected tracking error magnitudes computed by a pseudo–random process. Finally, if $|\bar{\delta}_1|$ is not increasing, the maneuver will not be computed. This prevents maneuvers from being implemented when the spacecraft is actually approaching the nominal trajectory (perhaps due to a previous maneuver). All of these criteria must be satisfied simultaneously for a maneuver to be computed and executed.

SOME RESULTS

The impact of a number of the quantifiable parameters on total mission cost has been considered in this investigation in conjunction with the effort to evaluate the Target Point and Floquet Mode station-keeping strategies. The final step in preparing both algorithms for evaluation is determination of input values for a "baseline case." For the Target Point method using constant weighting matrices, the inputs are first selected (by trial and error) with the sole purpose of successfully controlling the spacecraft without regard to maneuver costs. Then, the inputs are adjusted (again by trial and error) to reduce the total cost. When a set of input values produces an acceptable "minimum" cost, the set is specified as the "baseline" case. Parameters of interest can then be varied independently to investigate the impact on the performance of the station-keeping approach relative to the baseline case. Similar procedures are employed for the Floquet Mode approach.

Target Point Results

Values corresponding to the baseline inputs selected for the Target Point station-keeping strategy appear in Table 1. All three target points are used to compute the cost, and predicted errors at each target point are considered. Standard deviations for the error models are selected to correspond to those published in other works [4, 5, 6, 7]. All weighting matrices are diagonal. Units on elements of the weighting matrices are chosen to be consistent with velocity values in meters per second and position values in kilometers.

Using these inputs and this operational structure in the Target Point station-keeping algorithm, Monte Carlo simulations based on 100 trials are undertaken and baseline results are produced. To present output in an appropriate format, tabulated values corresponding to quantities useful in representing the vehicle maneuver history during the simulated mission are stored for each trial. Table 2 is a maneuver history representing one of the baseline trials. The first column of data indicates the time of the manuever relative to orbit injection, and the second column lists the number of days between consecutive maneuvers. Columns three through six contain the $x-$, $y-$, and $z-$components of the $\Delta\bar{v}$ maneuver and the maneuver magnitude, $|\Delta\bar{v}|$. The seventh column provides information about the "actual" maneuver error, and column eight is the magnitude of the position deviation relative to the nominal orbit at the time of the maneuver. The most successful trials never compute maneuvers with large components in the $z-$direction, and Table 2 supports this observation. This result is consistent across all simulations.

To obtain data that is more representative of the station-keeping performance, the results from the 100 trials are averaged. Statistics corresponding to the total cost and total number

Table 1: Baseline Input Values for the Target Point Strategy

Input	Baseline Value
Orbit injection date	July 1, 1995
p_{min}	0.0 km
t_{min}	30.0 days
v_{min}	2 $\frac{\text{cm}}{\text{s}}$
Target points weighted in position	3
Target points weighted in velocity	0
t_1, t_2, t_3	35.0, 65.0, 90.0 days
Mission duration	4.0 years
Tracking interval	2.0 days
Tracking and orbit injection errors: σ_x, σ_y, σ_z $\sigma_{x'}$, $\sigma_{y'}$, $\sigma_{z'}$	1.5 km, 2.5 km, 15 km, 1.0 $\frac{\text{mm}}{\text{s}}$, 1.0 $\frac{\text{mm}}{\text{s}}$, 3.0 $\frac{\text{mm}}{\text{s}}$
Maneuver errors: σ_{Δ_x}, σ_{Δ_y}, σ_{Δ_z}	2.5% of the planned $\lvert\Delta\bar{v}\rvert$
$\mathcal{Q}$ (nondimensional)	$diag[3.98 \times 10^{10}$ 4.92×10^{14} $1.30 \times 10^{13}]$
$\mathcal{R}$ $\left(\frac{1}{\text{s}^2}\right)$	$diag[2.90$ 2.80×10^{-2} $1.00 \times 10^{-3}]$
$\mathcal{S}$ $\left(\frac{1}{\text{s}^2}\right)$	$diag[4.40 \times 10^{-2}$ 1.00 $0.00]$
$\mathcal{T}$ $\left(\frac{1}{\text{s}^2}\right)$	$diag[3.00 \times 10^{-3}$ 9.30×10^{-2} $1.00 \times 10^{-1}]$

of maneuvers associated with the baseline case are listed below.

Total $\Delta\bar{v}$ cost:
Average $= 0.707 \frac{\text{m}}{\text{s}}$,
$\sigma^2 = 0.004 \left(\frac{\text{m}}{\text{s}}\right)^2$.

Number of maneuvers executed:
Average $= 26.6$,
$\sigma^2 = 3.63$.

Figure 2 is a more complete graphical representation of the data associated with the cost and number of maneuvers required for the baseline simulations. In the top plot, the abscissa variable reflects the number of simulations and the ordinate measures the total cost ($\Delta\bar{v}_T$ for each case), the cummulative average $\Delta\bar{v}_T$, and the "running" variance. The variance curve appears to approach a constant value after about 30 simulations which supports conclusions in [5]. However, as t_{min} is increased, the number of trials required to insure statistical significance of the average values increases as well.

Once the baseline case is established, numerical studies of the impact of some quantifiable parameters on station-keeping performance are structured so that only the particular parameter of interest is varied with respect to the set of baseline inputs during any one simulation. Results from execution of the Target Point algorithm reveal no serious problems with sensitivities to numerical accuracies or parameter settings. Four parameters that influence the performance of the Target Point algorithm are investigated: t_{min}, v_{min}, mission

Table 2: Target Point Maneuver History[a]

Time (days)	Δt^c_{man} (days)	Δ_x ($\frac{m}{s}$)	Δ_y ($\frac{m}{s}$)	Δ_z ($\frac{m}{s}$)	$\lvert\Delta\bar{v}\rvert^b$ ($\frac{m}{s}$)	Maneuver Error (%)	$\lvert\bar{p}_c\rvert$ (km)
102.0	102.0	0.022	0.001	0.000	0.022	0.0059	26.66
134.0	32.0	0.028	0.002	0.000	0.028	0.5114	30.28
166.0	32.0	0.022	0.002	0.000	0.022	0.1180	28.95
226.0	60.0	0.022	-0.001	0.000	0.022	0.3316	47.05
268.0	42.0	-0.023	-0.001	0.000	0.023	0.2933	30.29
354.0	86.0	-0.023	0.000	0.000	0.023	0.2057	33.95
436.0	82.0	-0.021	-0.001	0.000	0.021	0.1980	15.41
466.0	30.0	0.034	0.001	0.000	0.034	0.5308	46.38
498.0	32.0	0.031	0.002	0.000	0.031	0.7098	42.98
530.0	32.0	0.020	0.002	0.000	0.021	0.1393	34.51
604.0	74.0	0.025	-0.001	0.000	0.025	0.1114	43.06
678.0	74.0	-0.021	0.001	0.000	0.021	0.1222	41.80
738.0	60.0	-0.022	0.000	0.000	0.022	0.3455	55.82
798.0	60.0	-0.021	-0.002	0.000	0.021	0.2111	29.24
828.0	30.0	0.036	0.001	0.000	0.036	0.0785	79.43
860.0	32.0	0.041	0.003	0.000	0.041	0.0258	61.18
892.0	32.0	0.020	0.003	0.000	0.021	0.1059	48.27
964.0	72.0	0.029	-0.002	0.000	0.030	0.8966	58.60
1044.0	80.0	0.031	0.003	0.000	0.031	0.1779	45.70
1148.0	104.0	-0.075	-0.004	0.000	0.075	0.6926	75.33
1180.0	32.0	0.021	-0.003	0.000	0.021	0.2504	65.42
1214.0	34.0	0.024	0.002	0.000	0.024	0.3534	130.39
1262.0	48.0	0.055	0.004	0.000	0.055	0.0056	36.62
1304.0	42.0	0.021	0.000	0.001	0.021	0.9109	97.25
1348.0	44.0	0.025	-0.002	0.000	0.026	0.8358	39.03
1396.0	48.0	0.023	0.002	0.000	0.023	0.6609	86.48

[a] Number of maneuvers executed: 26
[b] Total $\Delta\bar{v}$ cost = 0.740 $\frac{m}{s}$
[c] Average Δt_{man} = 55.5 days

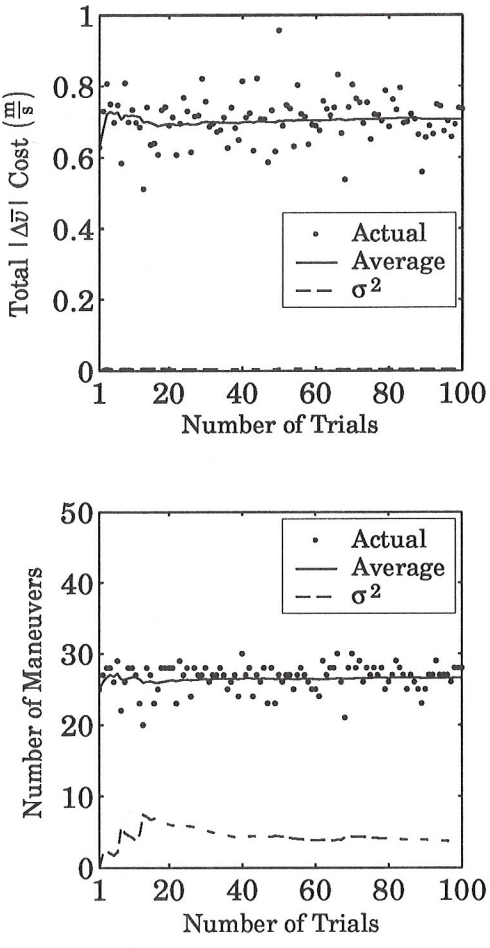

Figure 2: Baseline Case Results for the Target Point Strategy

Table 3: Results from Implementation of the Target Point Approach Using Constant Weighting Matrices

	$\Delta\bar{v}_T$ $(\frac{m}{s})$		n_{man}		Convergence
Input Parameters	Average	Variance	Average	Variance	(%)
t_{min}:					
† 30 days	0.707	0.004	26.6	3.63	100
40 days	0.829	0.008	25.0	3.69	100
50 days	1.04	0.013	22.6	1.86	100
80 days	5.54	2.49	17.5	0.372	100
90 days	37.5	388.0	16.0	0.033	88
v_{min}:					
0.00 $\frac{m}{s}$	0.650	0.001	42.2	1.49	100
† 0.02 $\frac{m}{s}$	0.707	0.004	26.6	3.63	100
0.04 $\frac{m}{s}$	1.03	0.005	23.1	1.98	100
p_{min}:					
† 0.0 km	0.707	0.004	26.6	3.63	100
50.0 km	0.985	0.013	24.7	3.41	100
100.0 km	1.80	0.039	22.4	3.57	100
t_{dur}:					
2.00 years	0.339	0.001	13.7	1.73	100
† 4.00 years	0.707	0.004	26.6	3.63	100
6.33 years	1.33	0.013	44.3	6.89	100

duration (t_{dur}), and p_{min}.

Results from station-keeping simulations using constant weighting matrices appear in Table 3. All numbers shown are averages based on 100 trials. The last column titled "Convergence (%)" indicates the number of trials that converge, that is, successfully control the spacecraft trajectory for the duration of the simulation, i.e., t_{dur}, using the specified input parameters. Thus, statistical computations are based only on the cases that converge. The input parameter t_{min} is one of the most crucial mission constraints. Apparently, as seen in Table 3, increasing t_{min} to 50, 80, or 90 days **may** have a significant impact on performance in terms of maneuvers costs. Not surprisingly, as t_{min} increases, $\Delta\bar{v}_T$ and the variance increase as well. Also, Δt_{man} approaches t_{min} for larger values of t_{min} (for cases that converge) as seen as below.

t_{min} (days)	Δt_{man} (days)
30.0	55.8
40.0	59.7
50.0	66.6
80.0	86.7
90.0	96.2

It is noted that the station-keeping strategy is fairly robust, i.e., the spacecraft can be maintained at 90 day intervals for a slight increase in cost. Of course, the resulting average value of n_{man} (number of maneuvers that are required) shows an inverse relationship to t_{min}; n_{man} decreases along with the variance. Of the three conditional statements, constraining the computation of maneuvers, t_{min} is often the last one satisfied.

Table 3 is somewhat misleading. A strong correlation between target point spacing and t_{min} can be demonstrated by adjusting the spacing between the target points to lower the cost; coupled with new weighting matrices, the new cost can be lower. As an example, consider the case in which $t_{min} = 80$ days. Modify the target point spacing such that input values for t_1, t_2, t_3 are 65 days, 66 days, and 131 days, respectively, and construct new weighting matrices. The average cost drops from 5.54 m/s to 2.10 m/s.

Although it is clearly beneficial, the large number of free parameters associated with the method (due, in part, to the weighting matrices) currently requires a significant amount of manual (trial and error) effort to minimize mission costs. Developed in this investigation is a method to automate selection of the weighting matrices, which greatly reduces manual efforts to establish control of the spacecraft path. Though the results obtained using time–varying matrices are slightly more costly than results produced with the constant matrices at this time, much user effort is saved and evidence suggests that the methodology can be improved in future investigations to eventually eliminate the need for manual selection of the weighting matrices. Another parameter that would benefit from automated optimization is the spacing of the target points; when various values of t_{min} (minimum time between maneuvers) are examined, shifting the target point locations can have a large impact on maneuver costs.

Floquet Mode Results

Baseline values similar to the Target Point baseline case were determined for the Floquet Mode approach. These inputs are determined by trial and error, with the initial goal being successful control of a spacecraft in orbit near a libration point for the specified mission duration. Next, the inputs are adjusted by trial and error to reduce the total cost levels to acceptable "minimum" values. The final result becomes the set of baseline input values.

Recall that two different types of Floquet controllers have been formulated (x-axis and three-axis). Table 4 contains the baseline input values and it is noted that all input values common to the Target Point and Floquet Mode algorithms are identical. Monte Carlo simulations based on 100 trials were produced for each baseline case. The results for the Floquet Mode baseline cases are tabulated and recorded in files that contain information about the maneuver histories. Table 5 is a sample maneuver history for one trail using the baseline inputs associated with three-axis control. The first column lists the time of each maneuver relative to the trajectory injection. The second and third columns include the magnitudes of the error vector (relative to the nominal orbit) and the corresponding unstable component of the error vector at the maneuver time. Columns four through seven list the x, y, and z components of the $\Delta\bar{v}$ maneuver and the maneuver magnitude, $|\Delta\bar{v}|$. Statistical data pertaining to each 100-trial Monte Carlo analysis is as follows:

Table 4: Baseline Input Values for the Floquet Mode Strategy

Input	Baseline Value
Orbit injection date	July 1, 1995
t_{min}	30.0 days
v_{min}	2 $\frac{cm}{s}$
$\|\delta_1\|_{min}$	1.74×10^{-10} (nondimensional)
Mission duration	4.0 years
Tracking interval	2.0 days
Tracking and orbit injection errors σ_x, σ_y, σ_z $\sigma_{x'}$, $\sigma_{y'}$, $\sigma_{z'}$	 1.5 km, 2.5 km, 15 km, 1.0 $\frac{mm}{s}$, 1.0 $\frac{mm}{s}$, 3.0 $\frac{mm}{s}$
Maneuver erros $\sigma_{\Delta x}$, $\sigma_{\Delta y}$, $\sigma_{\Delta z}$	 2.5 % of the planned $\|\Delta\bar{v}\|$
Controller type	X-axis control, Three-axis
Q for Three-Axis Controller (nondimensional)	*diag* [1.81 1.81 1.15 1.81 1.81 .120 30.1 356.0]

X–Axis Control

Total $\Delta\bar{v}$ cost:
Average $= 4.209 \frac{m}{s}$,
$\sigma^2 = 14.48 \left(\frac{m}{s}\right)^2$.

Number of maneuvers executed:
Average $= 38.5$,
$\sigma^2 = 12.0$.

Three–Axis Control

Total $\Delta\bar{v}$ cost:
Average $= 2.217 \frac{m}{s}$,
$\sigma^2 = 2.393 \left(\frac{m}{s}\right)^2$.

Number of maneuvers executed:
Average $= 35.2$,
$\sigma^2 = 15.1$.

Results from the two Floquet Mode controllers roughly correspond to published results (for similar input conditions and a nominal orbit similar in nature to the ISEE–3 halo orbit, assuming correct interpretation of the data). However, these references do not indicate that Monte Carlo procedures were employed for more than ten trials. Large variances in the data obtained in this investigation, then, make it difficult to ensure meaningful comparisons. Overall, the three–axis control strategy is superior to the x–axis controller. Therefore, the three–axis controller was chosen to represent the Floquet Mode station-keeping strategy. The average results produced using three-axis control are shown graphically in Fig. 3. Maneuver computations using three-axis control reveal (again) that the most successful trials have no $\Delta\bar{v}$ components in the z-direction. The increase in σ is noted. On the average, x-axis control is approximately 81% as effective as three-axis control.

Results from Monte Carlo simulations (each 100 trials) employing the Floquet Mode station-keeping strategy are summarized in Table 6. All operational conditions are consistent with those used for the Target Point approach.

Table 5: Floquet Mode Maneuver History Using Three-Axis Control[a]

Time (days)	Δt^c_{man} (days)	$\lvert\bar{\delta}\rvert$	$\lvert\bar{\delta}_1\rvert$	Δ_x $(\frac{m}{s})$	Δ_y $(\frac{m}{s})$	Δ_z $(\frac{m}{s})$	$\lvert\Delta\bar{v}\rvert^b$ $(\frac{m}{s})$
104.0	104.0	2.07×10^{-4}	2.01×10^{-4}	0.029	0.000	0.000	0.029
164.0	60.0	2.27×10^{-4}	1.78×10^{-4}	0.029	0.001	0.000	0.029
230.0	66.0	2.07×10^{-4}	1.77×10^{-4}	0.020	0.004	0.000	0.021
260.0	30.0	3.87×10^{-4}	3.42×10^{-4}	-0.042	-0.001	0.000	0.042
290.0	30.0	2.03×10^{-4}	1.89×10^{-4}	-0.031	0.001	0.000	0.031
328.0	38.0	2.61×10^{-4}	2.14×10^{-4}	-0.030	-0.008	0.000	0.031
358.0	30.0	2.88×10^{-4}	2.67×10^{-4}	-0.038	0.001	0.000	0.038
402.0	44.0	2.08×10^{-4}	1.87×10^{-4}	-0.023	-0.001	0.000	0.023
452.0	50.0	2.08×10^{-4}	1.89×10^{-4}	0.026	0.000	0.000	0.026
544.0	92.0	1.93×10^{-4}	1.88×10^{-4}	-0.027	0.002	0.000	0.027
600.0	56.0	2.24×10^{-4}	1.79×10^{-4}	0.020	0.003	0.000	0.020
630.0	30.0	4.86×10^{-4}	4.61×10^{-4}	-0.063	0.001	0.000	0.063
694.0	64.0	2.14×10^{-4}	1.92×10^{-4}	-0.028	-0.005	0.000	0.028
738.0	44.0	1.90×10^{-4}	1.77×10^{-4}	-0.024	0.001	0.000	0.024
780.0	42.0	2.14×10^{-4}	1.88×10^{-4}	0.023	0.000	0.000	0.023
890.0	110.0	3.13×10^{-4}	2.87×10^{-4}	-0.042	-0.001	0.000	0.042
986.0	96.0	2.73×10^{-4}	1.81×10^{-4}	-0.025	0.000	0.000	0.025
1054.0	68.0	2.38×10^{-4}	1.78×10^{-4}	-0.020	-0.003	0.000	0.020
1086.0	32.0	2.54×10^{-4}	1.81×10^{-4}	-0.025	0.002	0.000	0.025
1118.0	32.0	2.64×10^{-4}	1.78×10^{-4}	-0.021	-0.001	0.000	0.022
1148.0	30.0	4.51×10^{-4}	3.82×10^{-4}	-0.047	0.000	0.000	0.047
1178.0	30.0	4.18×10^{-4}	1.99×10^{-4}	-0.031	0.000	0.000	0.031
1208.0	30.0	5.58×10^{-4}	4.04×10^{-4}	-0.049	-0.007	0.000	0.049
1238.0	30.0	7.27×10^{-4}	6.43×10^{-4}	-0.027	-0.001	0.000	0.027
1268.0	30.0	1.83×10^{-3}	1.80×10^{-3}	-0.261	0.061	-0.002	0.268
1298.0	30.0	1.38×10^{-3}	1.32×10^{-3}	0.041	0.052	0.000	0.150
1328.0	30.0	2.37×10^{-3}	2.04×10^{-3}	-0.249	0.001	-0.009	0.250
1358.0	30.0	1.51×10^{-3}	1.24×10^{-3}	-0.213	0.023	0.001	0.214
1410.0	52.0	1.02×10^{-3}	2.28×10^{-4}	-0.020	-0.003	0.000	0.20
1440.0	52.0	1.52×10^{-3}	1.22×10^{-3}	-0.168	0.009	0.000	0.169

[a] Number of maneuvers executed: 35
[b] Total $\Delta\bar{v}$ cost $= 1.209\ \frac{m}{s}$
[c] Average $\Delta t_{man} = 41.1$ days

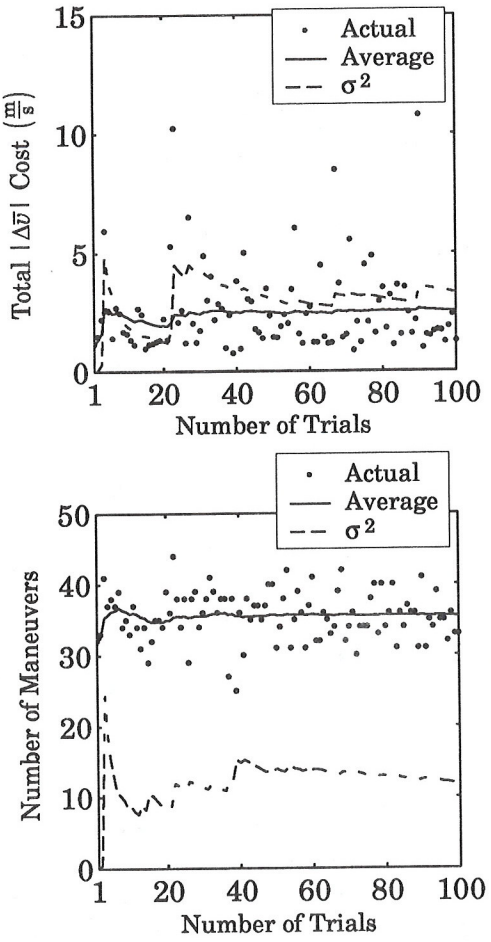

Figure 3: Baseline Case Results for the Floquet Mode Strategy Using Three–Axis Control

Of all parameters investigated, t_{min} clearly has the largest impact on the results in the Floquet Mode baseline case. Besides dramatic increases in cost, convergence even becomes a problem as t_{min} is increased. Average values for Δt_{man} are also close to t_{min}, i.e., for cases that converge,

t_{min} (days)	Δt_{man} (days)
30.0	42.7
40.0	47.6

The values for Δt_{man} are closer to the corresponding t_{min} values than those in the Target Point cases. Observation of the maneuver histories suggests that t_{min} is often the last condition satisfied before maneuver implementation, particularly for maneuvers in the later revolutions.

Table 6: Results from Implementation of the Floquet Mode Approach Using Three-Axis Control

	$\Delta\bar{v}_T\ (\frac{m}{s})$		n_{man}		Convergence
Input Parameters	Average	Variance	Average	Variance	(%)
t_{min}:					
† 30 days	2.22	2.39	30.9	5.60	100
40 days	47.1	2460	31.5	3.49	53
50 days	- -	- -	- -	- -	0
v_{min}:					
0.00 $\frac{m}{s}$	2.39	2.22	36.0	10.8	100
† 0.02 $\frac{m}{s}$	2.22	2.39	30.9	5.60	100
0.04 $\frac{m}{s}$	4.67	14.9	35.3	12.1	100
p_{min}:					
1.69×10^{-4}	2.34	2.31	35.9	10.9	100
‡ 1.74×10^{-4}	2.22	2.39	30.9	5.60	100
1.79×10^{-4}	2.47	2.85	35.9	11.5	100
t_{dur}:					
2.00 years	0.550	0.047	15.9	3.89	100
† 4.00 years	2.22	2.39	30.9	5.60	100
6.33 years	24.3	1450	61.0	23.6	100

Results from simulations using the Floquet Mode algorithm have demonstrated a need to reduce the number of computations that are currently required to implement the strategy. Sensitivities to numerical accuracies as well as computational costs are very high. These characteristics make manual optimization very time–consuming. In fact, station-keeping simulations employing the Floquet Mode approach require roughly five times as much computational time to implement than simulations using the Target Point algorithm. Nevertheless, implementation of the Floquet Mode strategy has been accomplished; some combination of parameters that results in successful control of the spacecraft in the vicinity of the nominal orbit have been determined. Continuing investigations of this station-keeping approach should initially focus on appropriate numerical issues.

V. SUMMARY

This work involves the implementation and analysis of two station–keeping strategies for spacecraft moving on a halo orbit in the vicinity of the interior L_1 libration point of the Sun–Earth–Moon system. Preliminary analysis completed in this investigation has identified several areas of concern and potential improvement for both methods.

Although the Target Point approach is much more efficient computationally, a clear advantage in favor of the Floquet Mode approach is the qualitative information and analysis made available through its implementation. For example, for a single trail the x–y projection of the nominal orbit appears in Fig. 4. Studies associated with the effectiveness of station–keeping maneuvers computed with the x–axis controller have indicated that

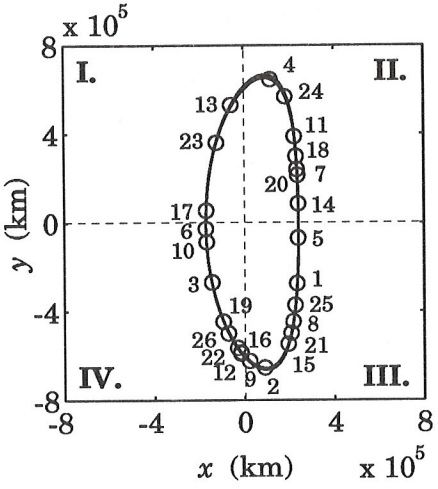

Figure 4: Quadrant Locations of Maneuvers

maneuvers are generally more effective in quadrants II and IV as defined in Fig. 4. The circles on the plot indicate locations of station–keeping maneuvers implemented in one of the Target Point baseline trials. Note, for example, how maneuvers "1" and "2," performed in quadrant III, result in maneuvers either in the same or neighboring quadrants. Maneuver "3," implemented in quadrant IV, however, is followed by a maneuver two quadrants away. Further support of this analysis is indicated by data from the ISEE–3 mission. With the exception of three maneuvers, all station–keeping maneuvers were implemented in quadrants II and IV. This is an excellent example of how the Floquet Mode approach can be used as a qualitative analysis tool to benefit both strategies.

With interest increasing in libration point trajectories, developments of these two strategies can be useful. The simplicity and robustness of the Target Point Method can complement the qualitative advantages of the Floquet Mode approach.

References

[1] Farquhar, R.W., "The Control and Use of Libration Point Satellites," NASA TR R-346, September 1970.

[2] Breakwell, J.V., Kamel, A.A., and Ratner, M.J., "Station-Keeping for a Translunar Communication Station," *Celestial Mechanics,* Vol. 10, No. 3, 1974, pp.357-373.

[3] Farquhar, R.W., Muhonen, D.P., Newman, C.R., and Heuberger, H.S., "Trajectories and Orbital Maneuvers for the First Libration-Point Satellite," *Journal of Guidance and Control,* Vol. 3, No. 6, 1980, pp.549-554.

[4] Howell, K.C., and Pernicka, H.J., "Stationkeeping Method for Libration Point Trajectories," *Journal of Guidance, Control, and Dynamics,* Vol. 16, No. 1, January-February 1993.

[5] Howell, K.C., and Gordon, S.C., "Orbit Determination Error Analysis and a Station-Keeping Strategy for Sun-Earth L_1 Libration Point Orbits," *The Journal of the Astronautical Sciences,* Vol. 42, No. 2, April-June 1994, pp. 207-228.

[6] Simó, C., Gómez, G., Llibre, J., and Martínez, R., "Station Keeping of a Quasiperiodic Halo Orbit Using Invariant Manifolds," *Proceedings of the Second International Symposium on Spacecraft Flight Dynamics,* Darmstadt, Germany, October 1986, pp. 65-70.

[7] Simó, C., Gómez, G., Llibre, J., Martínez, R., and Rodríquez, "On the Optimal Station Keeping Control of Halo Orbits," *Acta Astronautica*, Vol. 15, No. 6/7, 1987, pp. 391-397.

[5] Howell, K.C., and Gordon, S.C., "Orbit Determination Error Analysis and a Station-Keeping Strategy for Sun-Earth L_1 Libration Point Orbits," *The Journal of the Astronautical Sciences,* Vol. 42, No. 2, April-June 1994, pp. 207-228.

[6] Simó, C., Gómez, G., Llibre, J., and Martínez, R., "Station Keeping of a Quasiperiodic Halo Orbit Using Invariant Manifolds," *Proceedings of the Second International Symposium on Spacecraft Flight Dynamics,* Darmstadt, Germany, October 1986, pp. 65-70.

[7] Simó, C., Gómez, G., Llibre, J., Martínez, R., and Rodríquez, "On the Optimal Station Keeping Control of Halo Orbits," *Acta Astronautica*, Vol. 15, No. 6/7, 1987, pp. 391-397.